# The Exchangeable Yeast Ribosomal Acidic Protein YP2$\beta$ Shows Characteristics of a Partly Folded State under Physiological Conditions†

Jesús Zurdo,‡ Jesús M. Sanz,§ Carlos González,|| Manuel Rico,|| and Juan P. G. Ballesta*,‡

*Centro de Biología Molecular "Severo Ochoa" (CSIC-UAM), Universidad Autónoma de Madrid, 28049 Madrid, Centro de Investigaciones Biológicas (CSIC), Velázquez 144, 28006 Madrid, and Instituto de Estructura de la Materia (CSIC), Serrano 117, 28006 Madrid, Spain*

*Received January 31, 1997; Revised Manuscript Received May 29, 1997*⊗

ABSTRACT: The eukaryotic acidic ribosomal P proteins, contrary to the standard r-proteins which are rapidly degraded in the cytoplasm, are found forming a large cytoplasmic pool that exchanges with the ribosome-bound proteins during translation. The native structure of the P proteins in solution is therefore an essential determinant of the protein−protein interactions that take place in the exchange process. In this work, the structure of the ribosomal acidic protein YP2$\beta$ from *Saccharomyces cerevisiae* has been investigated by fluorescence spectroscopy, circular dichroism (CD), nuclear magnetic resonance (NMR), and sedimentation equilibrium techniques. We have established the fact that YP2$\beta$ bears a 22% α-helical secondary structure and a noncompact tertiary structure under physiological conditions (pH 7.0 and 25 °C); the hydrophobic core of the protein appears to be solvent-exposed, and very low cooperativity is observed for heat- or urea-induced denaturation. Moreover, the $^1$H-NMR spectra show a small signal dispersion, and virtually all the amide protons exchange with the solvent on a very short time scale, which is characteristic of an open structure. At low pH, YP2$\beta$ maintains its secondary structure content, but there is no evidence for tertiary structure. 2,2,2-Trifluoroethanol (TFE) induces a higher amount of α-helical structure but also disrupts any trace of the remaining tertiary fold. These results indicate that YP2$\beta$ may have a flexible structure in the cytoplasmic pool, with some of the characteristics of a "molten globule", and also point out the physiological relevance of such flexible protein states in processes other than protein folding.

To achieve a complete understanding of the mechanism of protein synthesis in the cell, detailed structural information of all the translation machinery components is required. Although considerable insight into the ribosome structure has been obtained using electron microscopy (Frank et al., 1995; Penczek et al., 1994) and there have been recent advances in crystallization (Evers et al., 1994; Yonath & Berkovitch-Yellin, 1993), a high-resolution three-dimensional structure of the particle is not yet available. In the meanwhile, the resolution of the tertiary structure of individual ribosomal components is providing relevant information on the architecture of the particle and its different functional domains (Davies et al., 1996a,b; Hoffman et al., 1996; Jaishree et al., 1996; Liljas & Garber, 1995; Nikonov et al., 1996).

One of the most characteristic ribosomal structures is the stalk, a highly flexible lateral protuberance on the large subunit (Marquis et al., 1981). The presence of the stalk has been reported in ribosomes from all the organisms examined (Lake, 1985), and it has been studied in some detail in *Escherichia coli*. The bacterial stalk has been found to be formed by two dimers of protein L7/L12, an N-terminal-blocked (L7) and an N-terminal-free (L12) polypeptide, and plays an important role in the activity of the supernatant factors during protein synthesis (Liljas & Gudkov, 1987; Möller & Maassen, 1986). Analogous ribosomal proteins have been found in all the studied species (Juan-Vidales et al., 1981). The equivalent proteins from eukaryotes display, however, some peculiarities that suggest additional functions in the regulation of the translation process [see Ballesta and Remacha (1996) for a review].

The stalk proteins are the only components present in multiple copies in the ribosome and are also the only ones that can be found free in the cytoplasm (Mitsui et al., 1988; van Agthoven et al., 1977; Zinker, 1980). These proteins have a molecular mass of around 12 kDa and an acidic isoelectric point ranging from 3 to 5. Only the structure of the *E. coli* L7/L12 protein has been studied in some detail (Liljas & Gudkov, 1987). The protein is present as a dimer in solution with well-defined C- and N-terminal domains joined by a "hinge" region. The C-terminal domain of L7/L12 forms the exposed tip of the stalk, while the N-terminal region interacts with the ribosome (Marquis et al., 1981; Olson et al., 1986) and is required for dimerization (Gudkov & Behike, 1978). Whereas the C-terminal region of L7/L12 has been crystallized and shown to have a compact structure with three α-helices and three antiparallel $\beta$-strands (Leijonmarck & Liljas, 1987), the remaining regions are less structured and could not be analyzed by X-ray diffraction methods. Evidence for the flexibility of the hinge region of

† This work was supported by Grants PB93-0189 and PB94-0032 from the Dirección General de Política Científica (Spain), by a grant from the Consejo Superior de Investigaciones Científicas, and by an institutional grant to the Centro de Biología Molecular from the Fundación Ramón Areces (Madrid).

* Address correspondence to J. P. G. Ballesta, Centro de Biología Molecular "Severo Ochoa" (CSIC-UAM), Fac. Ciencias, Universidad Autónoma de Madrid, Cantoblanco, E-28049 Madrid, Spain. Telephone: +34-1-3975076, Fax: +34-1-3974799. E-mail: jpgballesta@trasto.cbm.uam.es.

‡ Centro de Biología Molecular "Severo Ochoa".

§ Centro de Investigaciones Biológicas.

|| Instituto de Estructura de la Materia.

⊗ Abstract published in *Advance ACS Abstracts,* July 15, 1997.

S0006-2960(97)00240-7 CCC: $14.00 

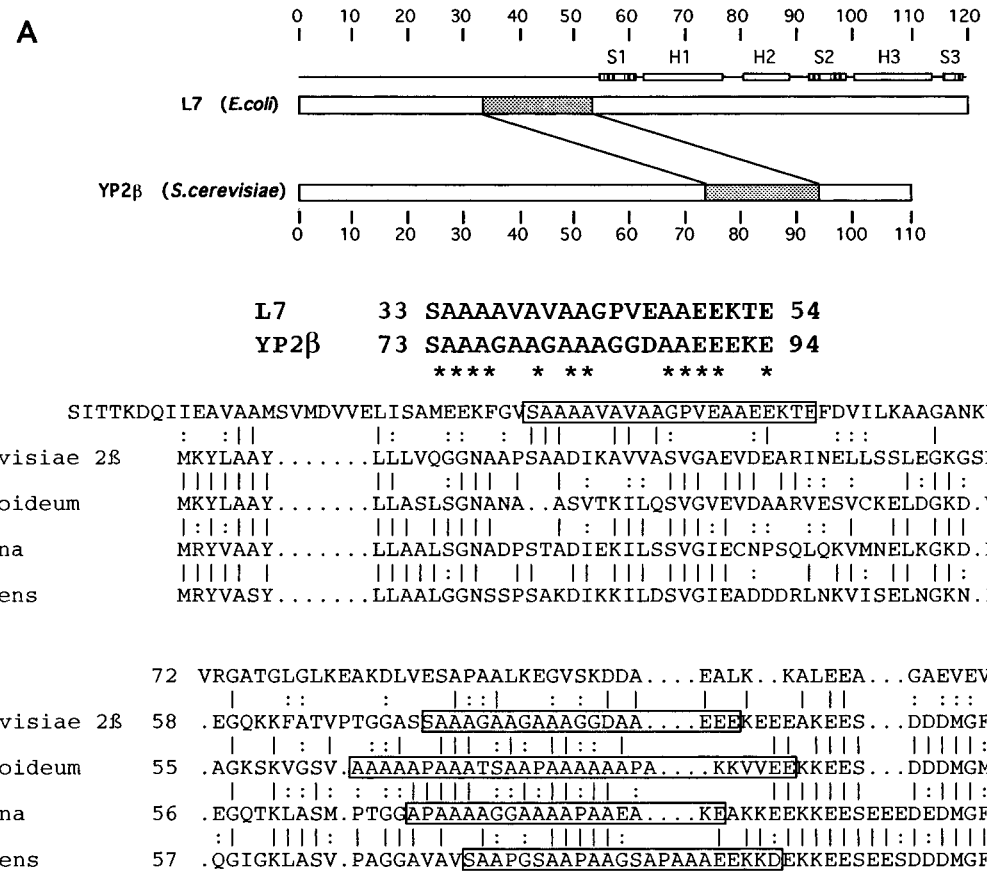


FIGURE 1: Sequence comparison between the prokaryotic L7/L12 protein and the eukaryotic P2 family. (A) Homologous regions in L7/L12 and YP2$\beta$ proteins. The score was obtained with the SIM (Huang & Miller, 1991) and LALNVIEW (Duret et al., 1996) programs at the Expasy internet site (http://expasy.hcuge.ch). The shaded regions show a 57.1% amino acid identity (sequence alignment is shown below the general profile); a second homology region was found between YP2$\beta$ residues 14−35 and 97−118 from L7/L12 with a 36.4% identity, which is not included due to its proximity to the usually required confidence score limit (Rost & Valencia, 1996). S1−S3 and H1−H3 denote $\beta$-strands and α-helices, respectively, as deduced from the L7/L12 X-ray structure. (B) Best fitting of the complete sequence of the L7/L12 protein with some eukaryotic ribosomal acidic proteins belonging to the P2 group; the postulated hinge region is marked by a box. The alignment between sequences was obtained with the program PILEUP (Genetics Computer Group Inc., Madison, WI).

L7/L12 was obtained from fluorescence studies (Lee et al., 1981; Zantema et al., 1982) and NMR[1] spectroscopy (Cowgill et al., 1984; Gudkov et al., 1982), and this flexibility has been shown to be essential for protein activity (Kirsebom et al., 1986; Oleinikov et al., 1993). Recent studies, using heteronuclear NMR, confirmed that the hinge region is unstructured and indicate that the N-terminal region may contain some loosely packed secondary structure elements (Bocharov et al., 1996).

No structural data concerning eukaryotic ribosomal acidic proteins, generically called P proteins, are available. Although the amino acid sequence homology is high among the eukaryotic acidic proteins (the C-terminal decapeptide is identical in yeast and in human cells), it is rather low between the prokaryotes and eukaryotes (Shimmin et al., 1989). Sequence similarities between the prokaryotic (L7/L12) and the eukaryotic (YP2$\beta$) proteins are mainly restricted to the so-called hinge region (Figure 1), an alanine-enriched sequence which has been proposed as a highly flexible connecting region that confers functionality to the L7/L12 protein (see above). Moreover, their overall structures must be dissimilar since the relative sizes of their C- and N-terminal domains are quite different (Figure 1). The lack of high structural homology between the two proteins also supports the physiological differences in their "*modus operandi*", as mentioned previously. Thus, the eukaryotic acidic proteins are found phosphorylated in the cell but not the prokaryotic L7/L12. In addition, dephosphorylation abolishes the capacity of the eukaryotic proteins to reconstitute active ribosomes *in vitro* (Juan-Vidales et al., 1984; MacConnell & Kaplan, 1982), and in apparent agreement with this, the proteins in the cytoplasmic pool are found to be dephosphorylated (Zinker, 1980). Furthermore, an exchange between the proteins from the ribosome and cytoplasm has been found to be associated to the translation process (Tsurugi & Ogata, 1985; Zinker & Warner, 1976). This feature places the eukaryotic acidic ribosomal proteins in the middle of the way between typical ribosomal proteins and supernatant factors.

On the other hand, whereas the prokaryotic acidic protein is genetically unique, their eukaryotic counterparts are encoded by several independent genes. Two types are found in mammals, called P1 and P2, but the number is larger in lower eukaryotes [see Ballesta and Remacha (1996) for a review]. In yeast, four different P proteins have been found (Beltrame & Bianchi, 1990; Newton et al., 1990); two of them belong to the P1 family (YP1α and YP1$\beta$) and two to

[1] Abbreviations: bis-ANS, 1,1′-bis(4-anilino)naphthalene-5,5′-disulfonic acid; CD, circular dichroism; [Θ], molar ellipticity; IPTG, isopropyl $\beta$-D-thiogalactopyranoside; ($^1$H-)NMR, (proton) nuclear magnetic resonance; $\delta$, chemical shift; PMSF, phenylmethanesulfonyl fluoride; TFE, 2,2,2-trifluoroethanol.

the P2 family (YP2α and YP2$\beta$). YP1$\beta$, YP2α, and YP2$\beta$ were previously characterized as L44′, L44, and L45, respectively (Juan-Vidales et al., 1984). The four yeast acidic proteins do not have identical functional roles since they cannot substitute one for another (Remacha et al., 1990, 1995). In fact, the simultaneous presence of P1 and P2 proteins is required for *in vivo* ribosome binding (Remacha et al., 1992).

In this report, a structural characterization of the yeast ribosomal acidic protein YP2$\beta$ is described. Different biophysical methods have been used to obtain structural and dynamical information about YP2$\beta$. The eukaryotic protein is shown to be more flexible than its prokaryotic counterpart since no highly structured domain was found. In fact, the experimental data indicate that the protein resembles a "molten globule" under physiological conditions. This is relevant in understanding the structure−function relationships in these types of ribosomal components.

## MATERIALS AND METHODS

*Materials and Reagents*. Oligonucleotides were from ISOGEN. CM-Sepharose Fast Flow and DEAE-Sepharose Fast Flow were purchased from Pharmacia. Sephadex G100 was from Sigma. Urea was the ultrapure type from ICN. 1,1′-Bis(4-anilino)naphthalene-5,5′-disulfonic acid, dipotassium salt (bis-ANS), was purchased from Molecular Probes Inc. 2,2,2-Trifluoroethanol (TFE) was from Sigma. Deuterated HCl ($^2$HCl), NaOH (NaO$^2$H), and deuterated TFE (TFE-$d_3$) were from CIL (Cambridge Isotope Laboratories). Deuterated $H_2O$ ($^2H_2O$) was from M&G Chemicals. 3,3,3-Trimethylsilylpropionate (TSP) was from SIC (Stohler Isotope Chemicals). Isopropyl $\beta$-D-thiogalactopyranoside (IPTG) was from Biomol. Phenylmethanesulfonyl fluoride (PMSF), aprotinin, and leupeptin were from Sigma. Ultrafiltration microsep and macrosep tubes were from FILTRON.

*Expression and Purification of the Protein.* The yeast YP2$\beta$ gene (Remacha et al., 1988) was subcloned in the pT7-7 vector under the control of the T7 promoter and expressed in *E. coli* strain BL21(DE3)plac carrying the T7 polymerase gene under lac promoter control (Studier & Moffatt, 1986; Studier et al., 1990). The gene construct was checked by DNA sequencing. Cells were grown at 37 °C in TB medium (200 mg/L ampicillin) up to an $A_{600}$ of 2.0 and then induced with 0.4 mM IPTG for 30 min. Rifampicin was then added at a final concentration of 200 mg/L, and the incubation was continued for 45 min. Cells were harvested, resuspended in 40 mM Tris (pH 7.4) and 5 mM EDTA containing 1 mM PMSF, 0.3 $\mu$M aprotinin, and 1 $\mu$M leupeptin, and disrupted using a French Press (20 000 psi). The lysate was first centrifuged at 10000*g* for 20 min and then at 120000*g* for 2 h to eliminate cell debris. The clear lysate was passed through a CM-Sepharose column to retain basic proteins and the flow through fraction absorbed in DEAE-Sepharose. Protein was then eluted from the DEAE-Sepharose column using a 0 to 500 mM NaCl linear gradient in 20 mM Tris at pH 7.8. The YP2$\beta$ protein, detected using specific monoclonal antibodies (Vilella et al., 1991), elutes as two distinct peaks at 175 and 220 mM NaCl. The first peak was subsequently identified by Edman degradation and mass spectrometry as the native YP2$\beta$ protein and the second as its N-terminal-blocked form. The first peak was collected, concentrated by employing macrosep ultrafiltration tubes with an exclusion limit of 3 kDa, loaded onto a pre-equilibrated Sephadex G100 column, and eluted with 20 mM Tris and 2 M NaCl at pH 7.8. The YP2$\beta$ protein peak was dialyzed against 20 mM Tris at pH 7.8 and again eluted through a DEAE-Sepharose column employing the same gradient described above. The protein was finally dialyzed again against either 10 mM Tris at pH 7.8 or water (if subject to lyophilization). When necessary, buffer exchange and concentration of the protein were carried out in ultrafiltration tubes.

*Protein Analysis*. Automatic Edman degradation was carried out on an Applied Biosystems 473A protein sequencer in the Protein Chemistry Service (Centro de Biología Molecular "Severo Ochoa"). Electrophoresis and isoelectrofocusing were as described before (Juan-Vidales et al., 1984). Mass spectrometry measurements were on an electrospray mass spectrometer (Peptide and Nucleotide Laboratory, Department of Organic Chemistry, Universidad de Barcelona). Western blot assays and ELISA were carried out using a set of previously characterized specific monoclonal antibodies (Vilella et al., 1991). The preparation of the four native ribosomal acidic proteins from *Saccharomyces cerevisiae* ribosomes (SP fractions) was done as reported earlier (Sanchez-Madrid et al., 1979).

*Protein Quantification*. Protein concentrations were determined from the absorbance at 280 nm using an extinction coefficient of 2560 $M^{-1}$ $cm^{-1}$ in water, calculated from the amino acid composition of the protein (Gill & von Hippel, 1989).

*Circular Dichroism.* Circular dichroism (CD) spectra were collected on a Jasco J720 spectropolarimeter fitted with a thermostated cell holder and interfaced with a Neslab RTE-110 water bath. Isothermal wavelength spectra were acquired at a scan speed of 20 nm/min with a response time of 2 s and averaged over four scans at 25 °C. The protein was initially dissolved in 20 mM potassium phosphate, at pH 7.0 and the pH adjusted as required by adding either $H_3PO_4$ or NaOH; 20 mM glycine at pH 2.0 was used as a buffer in some CD experiments. Far-UV CD measurements were done using 40−60 $\mu$g/mL protein in either a 1 mm or 2 mm path cuvette. Near-UV CD spectra were obtained on a 1−2 mg/mL protein solution in a 10 mm path cuvette. Ellipticities ([Θ]) are expressed in units of deg $cm^2$ $dmol^{-1}$, using the mean residue concentration of the protein. Thermal denaturation experiments were performed using a heating rate of either 20 or 50 °C/h and a response time of 2 s. Thermal scans were collected from 5 to 85 °C in 2 mm cuvettes with a protein concentration of 40−60 $\mu$g/mL. The reversibility of the thermal transitions was checked by recording a new scan after cooling the thermally denatured sample and comparing it with the spectra obtained before heat denaturation.

The approximate α-helical content of the protein was estimated from its molar ellipticity at 222 nm ($[\Theta]_{222}$) according to eq 1 (Chen et al., 1974).

$$f_H = [\Theta]_{222}/[[\Theta]_{222}^{\infty}(1 - k/n)] \quad (1)$$

where $f_H$ is the α-helical fraction of the protein, $[\Theta]_{222}$ is the observed mean residue ellipticity at 222 nm, $[\Theta]_{222}^{\infty}$ is the mean ellipticity for an infinite helix at 222 nm (−34 500 deg $dmol^{-1}$ $cm^2$), $k$ is a wavelength-dependent constant (2.57

at 222 nm), and $n$ is the number of peptide bonds of the molecule (109 for YP2$\beta$).

*Fluorescence Spectroscopy*. Fluorescence experiments were performed on a Perkin-Elmer LS-50B spectrometer at 25 °C. The protein concentration was 60 $\mu$g/mL, and buffers were the same as in CD measurements. Intrinsic fluorescence spectra were recorded from 295 to 410 nm at a scan speed of 100 nm/min (slit of 10 nm) upon excitation at 275 nm (slit of 5 nm). Blanks without protein were subtracted from the spectra. Quenching experiments were carried out employing acrylamide previously equilibrated in the desired buffer. The protein concentration was typically 60 $\mu$g/mL, whereas the acrylamide concentration was varied over 0−200 mM. Quenching of the intrinsic tyrosine fluorescence of YP2$\beta$ by acrylamide was analyzed using eq 2 (Eftink & Ghiron, 1981) and eq 3 (Lehrer, 1971)

$$F_0/F = (1 + K_{sv}[Q]) \exp(V[Q]) \quad (2)$$

$$F/(F - F_0) = 1 + K_q^{eff}[Q] \quad (3)$$

where $F$ and $F_0$ are the fluorescence intensities in the presence and in the absence of quencher, respectively, [Q] is the quencher concentration, $K_{sv}$ is the Stern−Volmer constant for the collisional quenching process, $V$ is the static quenching constant, and $K_q^{eff}$ is the "effective" quenching constant (Lehrer, 1971).

bis-ANS binding studies were typically performed using a concentration of 30 $\mu$M bis-ANS and 60 $\mu$g/mL protein. Fluorescence emission spectra of the probe were collected from 400 to 650 nm (slit of 10 nm) at a scan speed of 100 nm/min using an excitation wavelength of 380 nm (slit of 5 nm).

*Sedimentation Equilibrium*. Sedimentation equilibrium experiments of YP2$\beta$ protein in 20 mM potassium phosphate (pH 7.0), 20 mM glycine (pH 2.0), and 30% TFE in 20 mM potassium phosphate (pH 7.0) (loading concentration of 1 mg/mL) were performed at various rotor speeds ranging from 8000 to 27 000 rpm at 25 °C (20000−45000 in 30% TFE sample) in an Optima XL-A analytical ultracentrifuge (Beckman Instruments Inc.). After equilibrium was reached, scans (10 averages, 0.001 cm step size) were taken at 276 nm. Whole-cell apparent weight-average molecular masses ($M^c_{w,a}$) were obtained by fitting individual data sets to a sedimentation equilibrium model for a single species, employing the programs XLAEQ and EQASSOC (supplied by Beckman). The partial specific volume of YP2$\beta$ was 0.726 cm$^3$/g, as calculated from its amino acid composition (Laue, 1992).

To explore the self-associating behavior of YP2$\beta$, sedimentation equilibrium experiments were performed at three loading protein concentrations (0.3, 1.0, and 3.0 mg/mL) and at three different speeds (20 000, 25 000, and 36 000 rpm at pH 7.0 and 11 000, 15 000, and 22 000 rpm at pH 2.0) (McRorie & Voelker, 1993). Samples were in 20 mM potassium phosphate buffer (pH 7.0) and 20 mM glycine (pH 2.0) at 25 °C. The absorbance of the three samples (0.3, 1.0, and 3.0 mg/mL) was monitored at 236, 273, and 288 nm, respectively. Base lines for each sample were obtained after high-speed centrifugation at 45 000 rpm. The dependence of the apparent weight-average molecular mass ($M_w$) on protein concentration was calculated from local slopes of transformed data (ln $C$ versus $r^2$) at defined radial distance intervals with the program MWPLOTZ. $M_w$ values were calculated by superimposing data sets obtained from different loading protein concentrations and centrifugation speeds and averaging over a defined concentration range. Models for self-association were fitted to the $M_w$ versus concentration data using the programs FASTMWN and FASTMW (programs MWPLOTZ, FASTMWN, and FASTMW were kindly supplied by A. Minton, NIH).

*Chemical Cross-Linking*. For chemical cross-linking, two samples with different protein concentrations (1.0 and 3.0 mg/mL) in 20 mM potassium phosphate buffer at pH 7.0 were incubated for 10 min at 25 °C in the presence of glutaraldehyde at 5 mM. The reaction was stopped by the addition of 3 volumes of 9:1 (v/v) acetone/acetic acid and keeping the samples at −20 °C for 30 min. Then, the samples were spun at 13 000 rpm for 15 min. The pellet was resuspended in SDS−PAGE loading buffer and analyzed by electrophoresis.

*Nuclear Magnetic Resonance Spectroscopy*. $^1$H-NMR experiments were carried out in a Bruker 600 MHz spectrometer. One-dimensional spectra were recorded at 25 °C with 16K data points and using presaturation to eliminate the water signal. Data were processed with the Bruker software UXNMR. The sample concentration was typically 1−2 mg/mL in one-dimensional experiments. $D_2O$ experiments were carried out with freshly prepared sample. The $H_2O$ sample was lyophilized and the protein resuspended in $D_2O$. To discard any artifact due to protein denaturation after lyophilization, an additional $^1$H/$^2$H exchange experiment was performed by resuspending lyophilized YP2$\beta$ in $H_2O$ and then diluting up to 20 times with $D_2O$. The collected spectra were identical to those recorded by the previous procedure.

## RESULTS

*Identity and Integrity of the Purified Protein*. The identity of the recombinant YP2$\beta$ protein was confirmed as follows. (i) N-Terminal sequencing by automatic Edman degradation, where the first five cycles yielded the sequence M-K-Y-L-A, which coincides with that of the native protein, was first (Remacha et al., 1988; Santos et al., 1993) (Figure 1). (ii) SDS gel electrophoresis and isoelectrofocusing experiments showed that the migration of the recombinant protein corresponds to that of the native dephosphorylated form of YP2$\beta$ (Juan-Vidales et al., 1984). (iii) Specific monoclonal antibodies to YP2$\beta$ cross-react with the purified polypeptide (data not shown). (iv) Mass spectrometry of the protein yielded a molecular mass of 11 053 Da, in accord with that calculated from the sequence of the native protein (11 050 Da) (Remacha et al., 1988). (v) The recombinant YP2$\beta$ protein is able to bind to and to reconstitute the activity of acidic protein deficient ribosomes (J. Zurdo, A. Jiménez-Díaz, and J. P. G. Ballesta, unpublished results).

The second species of YP2$\beta$ protein obtained as described in Materials and Methods has a molecular mass of 11 081 Da (from mass spectrometry), compatible with an N-terminal formylation (formyl group = 28 Da). The N-blocked state of the polypeptide is consistent with the inability to determine the amino acid sequence by automatic Edman degradation. The presence of this protein might be due to incomplete deformylation of the first methionine, as a result of high levels of protein expression.

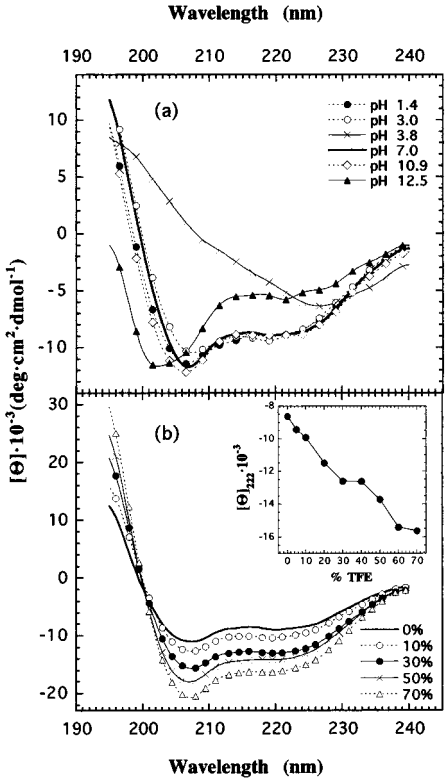


FIGURE 2: Far-UV CD spectra of YP2$\beta$. (a) Influence of pH on YP2$\beta$ far-UV CD spectra. The protein was incubated for 10 min at 25 °C in the desired buffer before spectra were recorded. The sample pH was adjusted by adding $H_3PO_4$ or NaOH to a 20 mM potassium phosphate buffer (pH 7.0); the protein was added at the end to avoid artifacts. In all cases, the pH was checked after the measurements were done to confirm its actual value. (b) Influence of TFE treatment on YP2$\beta$ far-UV CD spectra. Spectra were performed in 20 mM potassium phosphate buffer (pH 7.0), in the presence of different concentrations of TFE, expressed as a percentage (v/v). (Inset) Plot of $[\Theta]_{222nm}$ (in deg cm$^2$ dmol$^{-1}$ $\times$ $10^{-3}$) versus TFE percentage (v/v).

*Influence of Protein Concentration on YP2β Spectroscopic Features*. To assess the possible contribution of protein concentration to the spectroscopic measurements, CD and fluorescence signals were tested. Far-UV CD and fluorescence spectra were collected over a concentration range of 2−20 and 1−20 $\mu$M, respectively, whereas near-UV CD spectra were tested between 45 and 360 $\mu$M. In all cases, the intensities of the signals increase linearly with protein concentration (data not shown). Additionally, far-UV CD spectra of YP2$\beta$ at 90−180 $\mu$M recorded in a narrow-path (0.5 mm) cuvette were fitted to the linear regression established at lower protein concentrations. From these results, it can be concluded that, in these concentration ranges, the spectroscopic features of YP2$\beta$ are not influenced by protein concentration and therefore by possible aggregation phenomena.

*Circular Dichroism*. The effect of pH on the far-UV CD spectra of YP2$\beta$ is shown in Figure 2a. The far-UV CD spectrum at pH 7.0 displays two minima centered at 208 and 222 nm, characteristic of α-helical structure. This α-helical content, determined from the signal at 222 nm, is 22% (Chen et al., 1974). The spectra remain virtually invariable in the pH range of 1.5−11.0 but at a pH close to the calculated isoelectric point (4.1) (Bjellqvist et al., 1993) change, and the sample becomes turbid, indicating protein precipitation (pH 3.8 spectrum, Figure 2a). The appearance

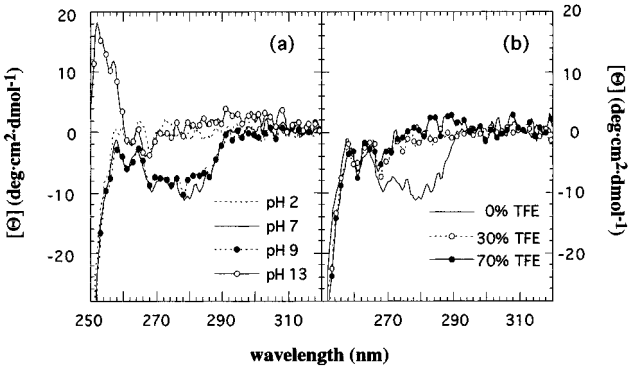


FIGURE 3: Influence of pH (a) and TFE concentration (b) on near-UV CD spectra of YP2$\beta$. Sample buffers were prepared as in Figure 2. For protein at pH 2, 20 mM glycine buffer (pH 2.0) was employed.

of a minimum at 200 nm at pH >12 indicates denaturation of the protein and the disappearance of the α-helical structure (Figure 2a). Addition of TFE increases continually the helical content of YP2$\beta$ up to 40% at 70% TFE (Figure 2b), although the titration curve does not reach a saturation phase (Figure 2b, inset).

Near-UV CD spectra provide information on the rigidity and environment of aromatic residues and can be used as an additional probe of protein structure. At neutral pH, the weak minimum centered at 280 nm (Figure 3a) indicates that the two tyrosines in YP2$\beta$, at positions 3 and 7, are in a somewhat constrained environment. However, this minimum disappears at pH 2.0, suggesting disruption of the tertiary folding of YP2$\beta$ around the tyrosine residues, although far-UV CD indicates no change in secondary structure (Figure 2a). Both far-UV and near-UV CD signals disappear at pH 13, consistent with global denaturation (see also Figure 2a). The near-UV CD signal, however, remains unaltered at basic pH values around 9.0 (Figure 3a). Nevertheless, TFE, which increases the α-helical content of YP2$\beta$ (Figure 2a), also causes the disappearance of the near-UV CD signal at 280 nm (Figure 3b). TFE ratios 30% and 70% henceforth chosen as representative TFE ratios from the intermediate and final regions of the titration curve (Figure 2b, inset).

*Intrinsic Fluorescence and Quenching Experiments*. The intrinsic fluorescence spectrum of the two tyrosines in YP2$\beta$ has a maximum centered at 306 nm that does not change either within pH 1.5−7.5 or at 7.5 M urea (Table 1). The fluorescence intensity is higher in the native protein and decreases slightly at low pH values (Table 1, data not shown) and substantially at 7.5 M urea (Table 1). These results are compatible with an exposure of both tyrosines to solvent on denaturation by acidic pHs or urea. Nevertheless, the contribution of proton quenching to the reduction in emission intensity observed at low pHs cannot be ruled out.

To explore the degree of solvent exposure of Tyr-3 and Tyr-7 in different conditions, quenching experiments with acrylamide were carried out. Data were analyzed by means of eqs 2 and 3 (Materials and Methods), and the effective Stern−Volmer quenching constant ($K_q^{eff}$) was considered a reliable measure of Tyr solvent exposure. $K_q^{eff}$ values were calculated considering the linear region of the $F_0/F$ versus acrylamide concentration plot (Eftink & Ghiron, 1981; Lehrer, 1971). The high $K_q^{eff}$ value obtained at pH 7.0 (25.1 $M^{-1}$) suggests significant solvent exposure of the tyrosines which is expected for a noncompact tertiary structure (Eftink

Table 1: YP2$\beta$ Tyrosine Intrinsic Fluorescence and bis-ANS Binding

| | sample[a] | $\lambda_{max}$ (nm) | relative emission[b] (arbitrary units) |
|---|---|---|---|
| intrinsic fluorescence | pH 7.0 | 306 | 100 |
| | pH 2.0 | 306 | 85 |
| | 7.5 M urea | 306 | 63 |
| bis-ANS binding | bis-ANS (pH 7.0) | 515.5 | 100[c] |
| | pH 7.0 | 494.5 | 671 |
| | pH 2.0 | 494.5 | 2743 |
| | urea 7.5 M | 515.5 | 157 |
| | pH 13.0 | 513 | 125 |
| | bis-ANS (30% TFE) | 519 | 100/269[d] |
| | 30% TFE | 517.5 | 104/279[d] |

[a] YP2$\beta$ was present in all the samples except in those noted as bis-ANS. [b] Emission of the protein and bis-ANS was considered 100% at pH 7.0. [c] bis-ANS emission at other pH values did not change significantly. [d] bis-ANS emission in TFE was considered either 100 or 269% (when normalized to bis-ANS emission at pH 7.0 in water).

& Ghiron, 1981). Quenching is somewhat increased at pH 2.0 ($K_q^{eff} = 31.2\ M^{-1}$) or in the presence of 7.5 M urea ($K_q^{eff} = 33.8\ M^{-1}$), possibly due to more extensive unfolding in these conditions, and agrees with near-UV CD measurements, showing disruption of the tertiary fold at acidic pH. On the other hand, the fact that $K_q^{eff}$ values for the protein in 7.5 M urea are different from those at pH 2.0 and at pH 7.0 supports the fact that the protein conformation at pH 2.0 or 7.0 is different from that of the urea-denatured protein.

*Bis-ANS Fluorescence.* The probe bis-ANS is used to monitor the solvent accessibility of hydrophobic patches in proteins. Partially folded states, molten globule structures, usually bind bis-ANS with high efficiency, causing an increase in the fluorescence of the molecule (Semisotnov et al., 1991). Protein YP2$\beta$ increases the bis-ANS emission at pH 7.0, indicating binding of the probe to the protein, whereas at pH 13.0 or in 7.5 M urea, conditions causing extensive unfolding of the protein, there is little effect on bis-ANS emission (Table 1). On the other hand, bis-ANS emission is much more enhanced at pH 2.0, suggesting an increased exposure of the protein hydrophobic cores to the solvent, although contribution from protein aggregation cannot be ruled out. Addition of 30% TFE to the protein causes no change in the bis-ANS fluorescence emission intensity (Table 1), consistent with alcohol-mediated unfolding.

*Thermal and Chemical Denaturation.* Figure 4 displays the thermal denaturation profiles of YP2$\beta$ at different pHs monitored by the ellipticity at 222 nm. At neutral pH, the CD signal intensity decreases above 30 °C with very low cooperativity; it is noteworthy that even at 85 °C the transition is not complete. The thermal transition at pH 2.0 is linear with temperature, suggesting the complete absence of cooperativity as would be expected for noncompact structure (Dobson, 1992). Thermal denaturation at pH 9.0 is similar to that at pH 7.0, but at pH >12, the transition resembles that of a random coil. These results point out the fact that the structure at pH 7.0 is stable up to a certain temperature and then disappears almost noncooperatively, suggesting both the existence of traces of rigid tertiary structure and the simultaneous presence of several conformers in equilibrium. Moreover, from the linear shape shown in Figure 4, it follows that YP2$\beta$ at pH 2.0 lacks specific

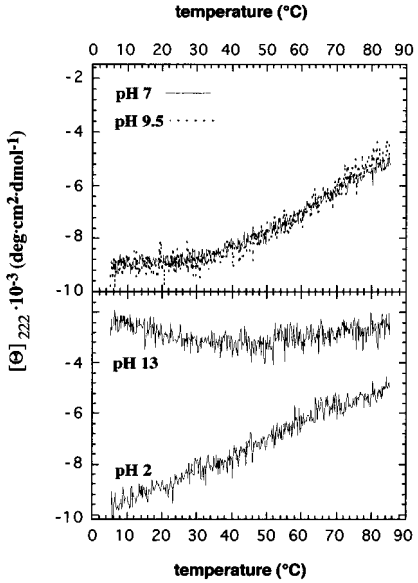


FIGURE 4: Thermal denaturation profiles of YP2$\beta$ at different pH values. Ellipticity at 222 nm was monitored as a function of temperature at the indicated pH. Buffers were as in Figure 3.

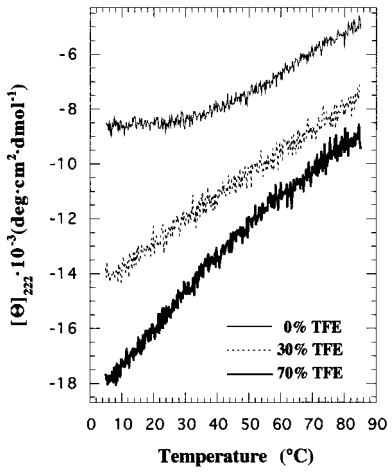


FIGURE 5: Thermal denaturation profiles of YP2$\beta$ in TFE. Ellipticity at 222 nm was monitored as a function of temperature at the indicated TFE rates. Buffers were as in Figure 3.

tertiary contacts at any temperature, even though some secondary structure is retained (at 85 °C, ellipticity at pH 2.0 is more intense than at pH 13). In the presence of TFE (Figure 5), the denaturation behavior of the protein is similar to the one observed at pH 2.0 (Figure 4), suggesting that, although the secondary structure is stabilized by TFE, the native tertiary fold is disrupted. These results agree with those from near-UV CD experiments since the disappearance of the tertiary fold correlates with the noncooperative thermal denaturation.

Urea denaturation of YP2$\beta$ at pH 7.0 shows a low cooperative broad transition (Figure 6), indicating that the unfolding equilibrium is likely to involve more than two states, and therefore is not amenable to determining protein stability. Urea denaturation at pH 2.0 is completely noncooperative as was seen in thermal denaturation experiments, in accordance with the complete lack of any residual tight structure at low pH (Figure 6). Moreover, at pH 2.0, there is a pronounced change in the slope at low denaturant concentrations (0.5 M urea) that could be explained by the disruption of protein aggregates (see below) by small

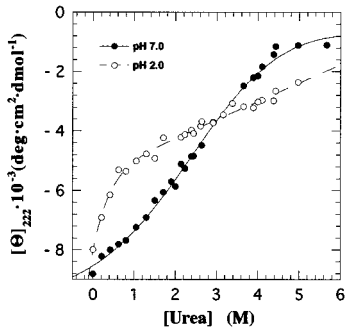


FIGURE 6: YP2$\beta$ urea denaturation. Ellipticity at 222 nm was monitored as a function of urea concentration at the indicated pH values.

amounts of urea. In this way, protein aggregation might stabilize the secondary structure content of the protein at such pH.

*Protein Aggregation*. To assess the molecular weight of the native protein and elucidate the existence of self-association phenomena, sedimentation equilibrium and chemical cross-linking studies were performed. Preliminary sedimentation equilibrium experiments at both pH 7 and 2 suggested that the protein appears to be polydisperse, since its apparent molecular weight ($M_w$) decreases with increasing rotor speed (Laue, 1992). To further study self-association, sedimentation assays at different speeds over a range of protein concentrations between 0.3 and 3.0 mg/mL were carried out. The increase in $M_w$[2] with protein concentration indicates the emergence of heavier species when the YP2$\beta$ concentration was increased, supporting the existence of a concentration-dependent self-associating system in equilibrium at both pH values (Figure 7a,b) (McRorie & Voelker, 1993).

Root-mean-square deviation (rmsd) criteria clearly rule out a simple equilibrium model for the self-associating behavior of the protein at pH 7.0. Nevertheless, a monomer−dimer−tetramer model can be fitted reasonably well to the experimental values of $M_w$ versus protein concentration at such a pH (Figure 7a), with the following equilibrium constants: $K_2 = 3.98 \times 10^4$ M$^{-1}$ and $K_4 = 3.24 \times 10^{13}$ M$^{-3}$. In order to confirm this model (monomer ↔ dimer ↔ tetramer equilibrium), cross-linking experiments were performed in the presence of glutaraldehyde and the products were resolved by SDS−PAGE. The presence of monomers, dimers, and tetramers was clearly visible in the gel (Figure 7E), whereas no trimer was detected. This excludes the involvement of trimers in the association equilibrium and confirms the monomer ↔ dimer ↔ tetramer equilibrium suggested by the sedimentation experiments. However, the proposed model is the simplest one that fits the experimental data, but the existence of additional species cannot be ruled out, especially at protein concentrations higher than those employed in the present sedimentation equilibrium analysis.

Some clear differences appear in the aggregation behavior exhibited by the protein at both pH values, since higher-$M_w$ species are detected at pH 2.0 (Figure 7a,b). This higher molecular weight exhibited by the protein aggregates at pH 2.0 is in accordance with a larger exposure of the protein hydrophobic patches (see above) that would promote an enhancement in the hydrophobic interactions between different polypeptide chains. Moreover, the simplest model that can be fitted to the experimental data at pH 2.0 is a 3mer ↔ 12mer equilibrium (Figure 7b) with a constant $K_{12}$ of $1.99 \times 10^{13}$ M$^{-9}$.

Interestingly, TFE modifies the self-association behavior of the protein, since the plot of $M^*_w$ (reference weight-average molecular mass)[3] versus protein concentration remains constant in the range tested (Figure 7a), as would be the case with a homogeneous sample (Laue, 1992). This result was confirmed by two additional observations. (i) The apparent molecular weight of YP2$\beta$ in 30% TFE remains virtually unchanged with the rotor speed, and (ii) the plot of ln $A$ (natural logarithm of absorbance) versus $r^2$ (square of radius) of YP2$\beta$ in 30% TFE fits a straight line (data not shown). Therefore, TFE prevents YP2$\beta$ aggregation.

Panels c and d of Figure 7 show the relative amount of each of the species involved in the observed equilibrium at pH 7.0 and 2.0, respectively. These data, joined to the fluorescence and CD studies at different protein concentrations described above, allow us to conclude that the spectroscopic properties of YP2$\beta$ do not change after self-association. In this way, at pH 7.0, these spectroscopic features can be assigned to the monomer and do not change after dimer and tetramer formation, since at the concentration ranges tested these three different species (monomer, dimer, and tetramer) exist in a concentration-dependent ratio (Figure 7c). On the contrary, contribution of aggregation to the denaturation profiles of the protein cannot be ruled out, and possibly, the lack of cooperativity observed may be influenced by the existence of several equilibrium conformations and/or aggregates (Ward et al., 1995).

*Nuclear Magnetic Resonance*. One-dimensional (1D) NMR spectra of YP2$\beta$ under native conditions (pH 7.0) show broad lines and a small chemical shift dispersion, in both the amide and methyl regions (Figure 8a). Despite the fact that pH- and TFE-induced differences in signal dispersion observed are not dramatic (Figure 8b,d−f), mainly because YP2$\beta$ does not show a large signal dispersion under native conditions, some correlation may be found between such spectral features and the structural changes associated with low pH and TFE treatment. In this way, signal dispersion is larger at neutral pH than at pH 1.9 (Figure 8a,b), consistent with other probes indicating the disruption of tertiary structure at low pH. Also, the higher signal broadening observed at pH 1.9 is in agreement with a larger size of protein aggregates, as was detected by analytical ultracentrifugation. NMR spectra in the range of pH of 3.0−5.0, close to the isoelectric point, showed very broad signals coincident with high turbidity (data not shown), indicating the presence of high-molecular weight aggregates.

The differences between the 1D NMR spectra of the native (Figure 8a) and the urea-denatured YP2$\beta$ protein (Figure 8c) confirm the existence of a partly structured state at pH 7 clearly different from a fully unfolded one. However, the broad signals shown by the protein and the lack of dispersion in chemical shifts prevented a complete assignment of the

[2] Figure 7 shows the relative $M_w$ normalized to the monomer mass ($M_w/M$).

[3] Since the effect of TFE/water mixtures on the partial specific volume ($\bar{\nu}$) of proteins is at present unknown, the term $M^*_w$ was employed instead of $M_w$ for graphical purposes. Thus, values of $\bar{\nu}$ and $\rho$ were arbitrarily taken from the protein in water (0.726 and 1.0, respectively) for $M^*_w$ calculations.

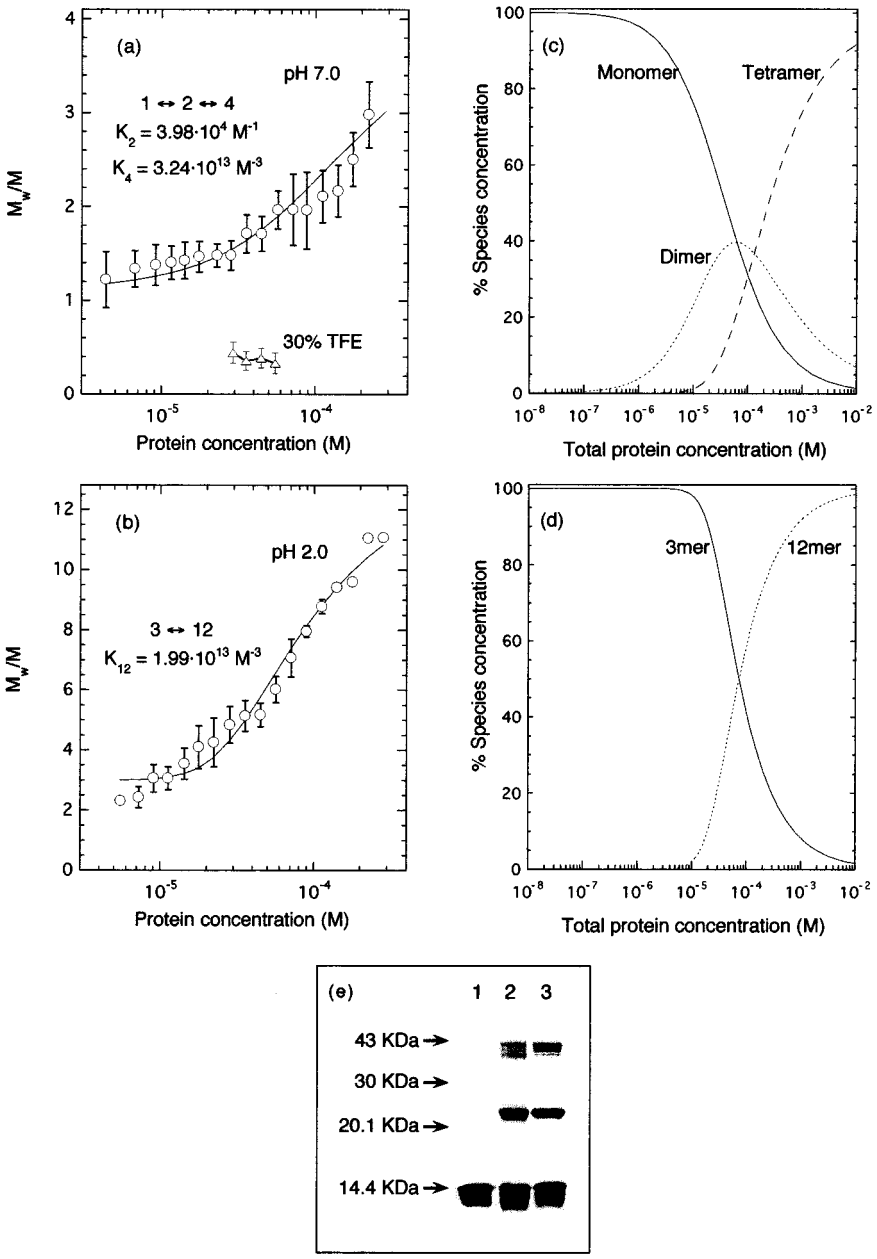


FIGURE 7: Self-association analysis of YP2$\beta$. (a and b) Relative weight-average molecular mass of YP2$\beta$ normalized to the monomer mass ($M_w/M$) plotted as a function of protein concentration ($C_{YP2\beta}$). Mean values plotted were obtained by averaging $M_w/M$ values each 0.1 unit of log($C_{YP2\beta}$) ($M$ units). A monomer ↔ dimer ↔ tetramer at pH 7.0 (a) or a 3mer ↔ 12mer equilibrium at pH 2.0 (b) was fitted to the experimental data to calculate the equilibrium constants ($K_2$, $K_4$, and $K_{12}$). The fit to such equilibrium is represented as a solid line. (c and d) Relative concentration of the species involved in the equilibrium versus total protein concentration at pH 7.0 (c) and pH 2.0 (d). (e) SDS−PAGE of YP2$\beta$ after chemical cross-linking in the presence of glutaraldehyde (lanes 2 and 3). Protein in the absence of the cross-linker is included (lane 1). Two different protein concentrations were employed: 1.0 mg/mL (lane 2) and 3.0 mg/mL (lane 3). Notice that the monomer shows an altered migration pattern.

spectra by 2D NMR methods. This evidence of a poorly defined structure in the core of the molecule is confirmed by the very rapid $^1H/^2H$ exchange observed in the amide region of the spectrum, which is virtually complete in 2 min (Figure 8g). The fact that all the amide protons of the protein exchange so quickly with solvent suggests that no stable tight structured region exists in the protein. Therefore, the secondary structure and tertiary fold of YP2$\beta$ are dynamic and fluctuating. The large line widths observed could thus be also due to conformational equilibrium between different states.

Figure 8 also shows the 1D NMR spectra of YP2$\beta$ at different TFE:$H_2O$ ratios. The line width of the proton resonances becomes sharper when TFE is added to the protein in a range between 15 and 30%. Higher concentrations of TFE (70%) slightly decrease chemical shift dispersion, so the spectrum becomes similar to the one in 7.5 M urea (Figure 8f). Two different effects of TFE on the sample would explain this behavior. (i) TFE could prevent protein aggregation, as seems possible from the sedimentation equilibrium assays (see above) which indicate the presence of a unique protein species (either monomeric or self-associating) that does not depend on protein concentration. (ii) As deduced from CD and bis-ANS binding experiments, TFE stabilizes the secondary structure content of YP2$\beta$ but, at the same time, disrupts the residual tertiary folding of the protein. The latter may explain why the chemical shift dispersion range decreases, while prevention of aggregation

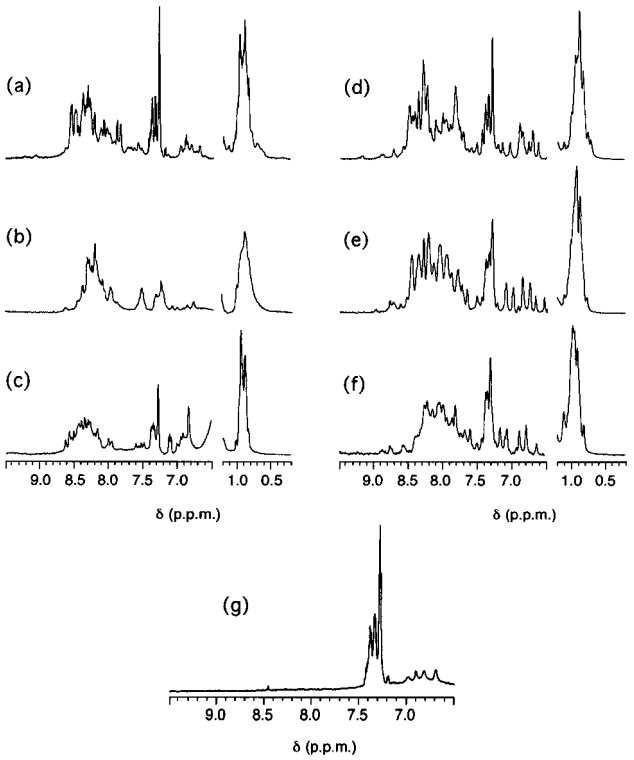


FIGURE 8: YP2$\beta$ NMR spectra. Effect of pH, chemical denaturation, and TFE on line width and chemical shift dispersion of YP2$\beta$ 1D-$^1$H-NMR spectra. Amide and methyl regions of the NMR spectra at pH 7.5 (a), pH 1.9 (b), 7.5 M urea (c), 15% TFE (d), 30% TFE (e), and 70% TFE (f) are presented. The TFE concentration is expressed as a percentage (v/v). (g) $^1$H/$^2$H exchange 1D-NMR. 1D-NMR spectra of YP2$\beta$ after 2 min of incubation in $^2H_2O$ at pH 6.4. Spectra were collected after 18 scans, and the acquisition time was 1 min.

by TFE may be responsible for the diminution of the signal broadness.

## DISCUSSION

The results presented in this work allow us to conclude that YP2$\beta$ is in a partly folded conformation under physiological conditions in the absence of other ribosomal components. This fact, joined to the aggregation exhibited by the protein (as pointed out by sedimentation equilibrium), hindered a detailed structural analysis by high-resolution methods. Instead, structural characterization of YP2$\beta$ was performed by several biophysical means, like CD, fluorescence spectroscopy, and 1D NMR.

Far-UV CD experiments show that the protein has up to 22% α-helical secondary structure which is stable at low pH and becomes higher with TFE. At neutral pH, the presence of some tertiary structure is indicated by the near-UV CD spectra, the chemical shift dispersion of the NMR signals, and the low cooperativity in the denaturation assays. However, the tertiary structure is not compact, and there is a partial exposure of the hydrophobic core to the solvent. bis-ANS binding experiments show that the hydrophobic core is accessible to the solvent at neutral pH, and more so at low pH. All the amide protons exchange with the solvent very rapidly, providing additional evidence of an exposed core of the protein. This also suggests that different fluctuating conformations exist in equilibrium under native conditions. Treatment with TFE clearly increases the α-helical content of YP2$\beta$ but, at the same time, disrupts its residual tertiary fold, suggesting that although secondary structure elements are stabilized they do not pack to form a hydrophobic core. In this way, the observed effect of TFE on the YP2$\beta$ structure agree with the postulated mechanism of action of some alcohols on protein solutions, enhancing local interactions but weakening long range interactions (Thomas & Dill, 1993).

The results obtained from all the different techniques indicate that, although YP2$\beta$ has a certain degree of secondary and tertiary structure at neutral pH, it lacks the usual rigidity of the completely folded proteins. These features strongly suggest that YP2$\beta$ shows a native conformation with some of the characteristics of a so-called molten globule (Bychkova & Ptitsyn, 1993; Dobson, 1992). Moreover, it is remarkable that the flexible character of YP2$\beta$ protein is displayed under physiological conditions, i.e. pH 7.0 and 25 °C, and in the absence of either chemical denaturants or organic solvents. Besides the basic interest that partly folded states have with respect to the protein folding problem from the physicochemical point of view, the relevance of "flexible states" *in vivo* is a subject of increasing interest.

Although the structural data described above depict the structure of YP2$\beta$ as a loosely packed polypeptide that bears a relatively exposed and fluctuating hydrophobic core and a substantial amount of secondary structure (all characteristics that define the molten globule state), some data also diverge from those exhibited by the "canonical" molten globule. The most important one is that the molten globule state is described as an equilibrium state that shows an all-or-none transition to the unfolded state (Ptitsyn, 1995), whereas native YP2$\beta$ displays a low cooperative transition to a fully unfolded state, which would agree better with a structurally fluctuating protein. Nevertheless, some authors have described molten globules without such cooperative transitions to unfolded states, arguing that the absence of a unique and tight tertiary structure in such states (although some tertiary fold could be present) agrees with a non-first-order transition (Schumann & Jaenicke, 1993). It is, however, clear that YP2$\beta$ is a partly folded protein that displays at least some of the features of molten globules.

The presence of partly folded proteins and/or disordered domains under native conditions is becoming important for several biological processes. Thus, protein ordering has been described upon specific DNA binding (Weiss et al., 1990; Zhao et al., 1993), involving formation of α-helices from disordered regions in the free state and quaternary rearrangements (Spolar & Record, 1994). On the basis of these results, the existence of a molten globule-like conformation for these proteins in the absence of DNA has been proposed (Hornby et al., 1994). Moreover, the existence of such partly folded domains and proteins is not restricted to DNA-binding proteins. For example, active transcription activation domains have a disordered conformation in the absence of their ligands (Dahlman-Wright et al., 1995; Donaldson & Capone, 1992; Schmitz et al., 1994). It is important to note that most of these largely unstructured domains in native-like conditions are acidic, as occurs with the P1 and P2 eukaryotic ribosomal proteins. Nevertheless, some nonacidic transcription activation domains seem to be also extensively unstructured (Cho et al., 1996).

Interestingly, examples of an active flexible conformation are appearing in proteins not directly related to transcription

regulation. Thus, some discrepancies between different crystal structures as well as NMR spectroscopy data led Hua and co-workers to postulate a molten globule state for the biologically active molecule of insulin (Hua et al., 1992, 1993).

From evidence such as this, an important role for flexible proteins in the physiological processes of the cell can be inferred. Some hypotheses have been formulated to explain the role of disordered conformations on cell biology. The "induced fit" mechanism (Ikura et al., 1992; Weiss et al., 1990) proposes that the protein (or domain) will reach its definitive conformation only after interaction with the ligand; the interaction, by reducing the kinetic barriers in the assembly of the complex, favors its formation (Weiss et al., 1990). On the other hand, the so-called "polypeptide lasso" model (Cho et al., 1996) postulates that the lack of a unique and tight structure makes these proteins more versatile in the interaction with different ligands which forms complexes with distinct activities and can allow the production of a higher variety of effects. In this way, conformational disorder has been correlated with binding diversity in proteins involved in cell cycle control (Kriwacki et al., 1996). Thus, the flexible state of "free YP2$\beta$" would acquire a tighter conformation after ribosome binding and/or interaction with other acidic proteins in forming the stalk. This would open new perspectives in the regulation of translation by conformational changes of proteins which involves partial unfolding. Moreover, a polypeptide lasso model would allow a control mechanism by the acidic proteins, enabling a number of possible interactions with other ligands (elongation factors, other acidic proteins, etc.) in order to regulate translation in response to different stimuli, as has been postulated for the acidic ribosomal proteins (Ballesta & Remacha, 1996). Thus, the flexible state of YP2$\beta$ could be a requirement for its interaction with other translational machinery components.

The high observed tendency of YP2$\beta$ to form aggregates would be *a priori* an obstacle for the normal functionality of the protein, taking into account the fact that an important part of acidic ribosomal protein pool in eukaryotic cells is free in the cytoplasm (not bound to ribosomes). This is particularly important because of the exchange between both fractions during translation (Tsurugi & Ogata, 1985; Zinker & Warner, 1976). Nevertheless, since it has been shown that chaperones specifically recognize the molten globule state, preventing aggregation (Bychkova & Ptitsyn, 1993), a way to explain the specificity of acidic protein interactions with the ribosome and other translation factors would be the transient binding to molecular chaperones. There is previous evidence indicating that acidic ribosomal proteins in the cytoplasm seem to be associated with high-molecular weight complexes (Remacha et al., 1992), compatible with their interaction with chaperone-like proteins.

It has to be noted, however, that even when bound to the ribosome the acidic proteins seem to have a certain degree of flexibility. 1D NMR experiments carried out on whole ribosomes detected relatively sharp resonances (Cowgill et al., 1984) which were attributed to the high mobility of the so-called hinge region of the bacterial protein L7/L12. These authors, in similar studies with yeast ribosomes, proposed that the acidic ribosomal proteins are the source of those signals in eukaryotic ribosomes (Cowgill et al., 1984). Since YP2$\beta$ ribosome binding also occurs through its N-terminal region (Payo et al., 1995) (and we were not able to detect any tight domain in the overall protein), these NMR signals in the yeast ribosome must be due to the flexibility of the acidic protein part comprising the hinge region and the C-terminal domain. Its extremely acidic character and small size (Figure 1) argue against a close conformation for the C-terminal eukaryotic domain and support its high flexibility even when bound to the ribosome.

Our results stress the important structural differences between prokaryotic and eukaryotic acidic ribosomal proteins. The presence of a compact domain has not been detected in YP2$\beta$, and this difference is even more striking if the fact that the structured C-terminal domain of L7/L12 protein comprises 74 residues out of the total 120 is considered, which constitutes the larger part of the polypeptide. These structural disparities support functional divergences, and in this respect, it is important to note that an exchange between the proteins in the ribosome and in the cytoplasm has not been reported for L7/L12, suggesting that the regulatory role postulated for the eukaryotic ribosomal components does not exist in eubacteria. Interestingly, although there are no experimental data on the existence of either a cytoplasmic pool of acidic proteins or an exchange process with the ribosome on archeabacteria, the archea acidic ribosomal proteins seem to be structurally closer to the eukaryotic than to the eubacterial polypeptides (Shimmin & Dennis, 1989).

## ACKNOWLEDGMENT

We thank M. Pavon for the initial cloning of the YP2$\beta$ gene in the pT7-7 vector, Dr. G. Rivas for help with acquisition and analysis of sedimentation equilibrium data, and M. C. Fernández for technical support. We also thank Dr. G. Giménez-Gallego for allowing the use of his fluorometer.

## REFERENCES

Ballesta, J. P. G., & Remacha, M. (1996) *Prog. Nucleic Acid Mol. Biol. 55*, 157−193.

Beltrame, M., & Bianchi, M. E. (1990) *Mol. Cell. Biol. 10*, 2341−2348.

Bjellqvist, B., Hughes, G. J., Pasquali, C., Paquet, N., Ravier, F., Sánchez, J.-C., Frutiger, S., & Hochstrasser, D. F. (1993) *Electrophoresis 14*, 1023−1031.

Bocharov, E. V., Gudkov, A. T., & Arseniev, A. S. (1996) *FEBS Lett. 379*, 291−294.

Bychkova, V. E., & Ptitsyn, O. B. (1993) *Chemtracts: Biochem. Mol. Biol. 4*, 133−163.

Chen, Y.-H., Yang, J. T., & Chau, K. H. (1974) *Biochemistry 13*, 3350−3359.

Cho, H. S., Liu, C. W., Damberger, F. F., Pelton, J. G., Nelson, H. C. M., & Wemmer, D. E. (1996) *Protein Sci. 5*, 262−269.

Cowgill, C. A., Nichols, B. G., Kenny, J. W., Butler, P., Bradbury, E. M., & Traut, R. R. (1984) *J. Biol. Chem. 259*, 15257−15263.

Dahlman-Wright, K., Baumann, H., McEvwan, I. J., Almlöf, T., Wright, A. P. H., Gustafsson, J.-A., & Härd, T. (1995) *Proc. Natl. Acad. Sci. U.S.A. 92*, 1699−1703.

Davies, C., Ramakrishnan, V., & White, S. W. (1996a) *Structure 4*, 1093−1104.

Davies, C., White, S. W., & Ramakrishnan, V. (1996b) *Structure 4*, 55−66.

Dobson, C. M. (1992) *Curr. Opin. Struct. Biol. 2*, 6−12.

Donaldson, L., & Capone, J. P. (1992) *J. Biol. Chem. 267*, 1411−1414.

Duret, L., Gasteiger, E., & Pierre, G. (1996) *Comput. Appl. Biosci. 12*, 507−510.

Eftink, M. R., & Ghiron, C. A. (1981) *Anal. Biochem. 114*, 199−227.

Evers, U., Franceschi, F., Boddeker, N., & Yonath, A. (1994) *Biophys. Chem. 50*, 3−16.
Frank, J., Zhu, J., Penczek, P., Li, Y., Srivastava, S., Verschoor, A., Radermacher, M., Grassucci, R., Lata, R. K., & Agrawal, R. K. (1995) *Nature 376*, 441−444.
Gill, S. C., & von Hippel, P. V. (1989) *Anal. Biochem. 182*, 319−326.
Gudkov, A. T., & Behike, J. (1978) *Eur. J. Biochem. 90*, 309−312.
Gudkov, A. T., Gongazde, G. M., Bushuev, V. N., & Okon, M. S. (1982) *FEBS Lett. 138*, 229−232.
Hornby, D. P., Whitmarsh, A., Pinarbasi, H., Kelly, S. M., Price, N. C., Shore, P., Baldwin, G. S., & Waltho, J. (1994) *FEBS Lett. 355*, 57−60.
Hua, Q. X., Kochoyan, M., & Weiss, M. A. (1992) *Proc. Natl. Acad. Sci. U.S.A. 89*, 2379−2383.
Hua, Q. X., Ladbury, J. E., & Weiss, M. A. (1993) *Biochemistry 32*, 1433−1442.
Huang, X., & Miller, W. (1991) *Adv. Appl. Math. 12*, 337−357.
Ikura, M., Clore, G. M., Gronenborn, A. M., Ahu, G., Klee, C. B., & Bax, A. (1992) *Science 256*, 632−638.
Jaishree, T. N., Ramakrishnan, V., & White, S. W. (1996) *Biochemistry 35*, 2845−2853.
Juan-Vidales, F., Sanchez-Madrid, F., & Ballesta, J. P. G. (1981) *Biochim. Biophys. Acta 656*, 28−35.
Juan-Vidales, F., Saenz-Robles, M. T., & Ballesta, J. P. G. (1984) *Biochemistry 23*, 390−396.
Kirsebom, L. A., Amons, R., & Isaksson, L. A. (1986) *Eur. J. Biochem. 156*, 669−675.
Kriwacki, R. W., Hengst, L., Tennant, L., Reed, S. I., & Wright, P. E. (1996) *Proc. Natl. Acad. Sci. U.S.A. 93*, 11504−11509.
Lake, J. A. (1985) *Annu. Rev. Biochem. 54*, 507−530.
Laue, T. M. (1992) *Short column sedimentation equilibrium analysis for rapid characterization of macromolecules in solution, Technical Information DS-835*, Spinco Business Unit, Palo Alto, CA.
Lee, C.-C., Wells, B. D., Fairclough, R. H., & Cantor, C. R. (1981) *J. Biol. Chem. 256*, 49−53.
Lehrer, S. S. (1971) *Biochemistry 10*, 3254−3263.
Leijonmarck, M., & Liljas, A. (1987) *J. Mol. Biol. 195*, 555−580.
Liljas, A., & Gudkov, A. T. (1987) *Biochimie 69*, 1043−1047.
Liljas, A., & Garber, M. (1995) *Curr. Opin. Struct. Biol. 5*, 721−727.
MacConnell, W. P., & Kaplan, N. O. (1982) *J. Biol. Chem. 257*, 5359−5366.
Marquis, D. M., Fahnestock, S. R., Henderson, E., Woo, D., Schwinge, D., Clark, M., & Lake, J. A. (1981) *J. Mol. Biol. 150*, 121−132.
McRorie, D. K., & Voelker, P. J. (1993) *Self-associating systems in the analytical ultracentrifuge*, Spinco Business Unit, Palo Alto, CA.
Mitsui, K., Nakagawa, T., & Tsurugi, K. (1988) *J. Biochem. 104*, 908−911.
Möller, W., & Maassen, J. A. (1986) in *Structure, function and genetics of ribosomes* (Hardestyand, B., & Kramer, G., Eds.) pp 309−325, Springer-Verlag, New York.
Newton, C. H., Shimmin, L. C., Yee, J., & Dennis, P. P. (1990) *J. Bacteriol. 172*, 579−588.
Nikonov, S., Nevskaya, N., Eliseikina, I., Fomenkova, N., Nikulin, A., Ossina, N., Garber, M., Jonsson, B. H., Briand, C., Al, K. S., Svensson, A., Aevarsson, A., & Liljas, A. (1996) *EMBO J. 15*, 1350−1359.
Oleinikov, A. V., Perroud, B., Wang, B., & Traut, R. R. (1993) *J. Biol. Chem. 268*, 917−922.
Olson, H. M. K., Sommer, A., Tewari, D. S., Traut, R. R., & Glitz, D. G. (1986) *J. Biol. Chem. 261*, 6924−6932.
Payo, J. M., Santana-Roman, H., Remacha, M., Ballesta, J. P. G., & Zinker, S. (1995) *Biochemistry 34*, 7941−7948.
Penczek, P. A., Grassucci, R. A., & Frank, J. (1994) *Ultramicroscopy 53*, 251−270.
Ptitsyn, O. B. (1995) *Curr. Opin. Struct. Biol. 5*, 74−78.
Remacha, M., Saenz-Robles, M. T., Vilella, M. D., & Ballesta, J. P. G. (1988) *J. Biol. Chem. 263*, 9094−9101.
Remacha, M., Santos, C., & Ballesta, J. P. G. (1990) *Mol. Cell. Biol. 10*, 2182−2190.
Remacha, M., Santos, C., Bermejo, B., Naranda, T., & Ballesta, J. P. G. (1992) *J. Biol. Chem. 267*, 12061−12067.
Remacha, M., Jimenez-Diaz, A., Bermejo, B., Rodriguez-Gabriel, M. A., Guarinos, E., & Ballesta, J. P. G. (1995) *Mol. Cell. Biol. 15*, 4754−4762.
Rost, B., & Valencia, A. (1996) *Curr. Opin. Biotechnol. 7*, 457−461.
Sanchez-Madrid, F., Reyes, R., Conde, P., & Ballesta, J. P. G. (1979) *Eur. J. Biochem. 98*, 409−416.
Santos, C., Ortiz-Reyes, B. L., Naranda, T., Remacha, M., & Ballesta, J. P. G. (1993) *Biochemistry 32*, 4231−4236.
Schmitz, M. L., dos Santos Silva, M. A., Altmann, H., Czisch, M., Holak, T. A., & Baeuerle, P. A. (1994) *J. Biol. Chem. 269*, 25613−25620.
Schumann, J., & Jaenicke, R. (1993) *Eur. J. Biochem. 213*, 1225−1233.
Semisotnov, G. V., Rodionova, N. A., Razgulyaev, O. I., Uversky, V. N., Gripas, A. F., & Gilmanshin, R. I. (1991) *Biopolymers 31*, 119−128.
Shimmin, L. C., & Dennis, P. P. (1989) *EMBO J. 8*, 1225−1235.
Shimmin, L. C., Ramirez, G., Matheson, A. T., & Dennis, P. P. (1989) *J. Mol. Evol. 29*, 448−462.
Spolar, R. S., & Record, M. T. (1994) *Science 263*, 777−784.
Studier, F. W., & Moffatt, B. A. (1986) *J. Mol. Biol. 189*, 113−130.
Studier, F. W., Rosenberg, A. H., Dunn, J. J., & Dubendorff, J. W. (1990) *Methods Enzymol. 185*, 60−89.
Thomas, P. D., & Dill, K. A. (1993) *Protein Sci. 2*, 2050−2065.
Tsurugi, K., & Ogata, K. (1985) *J. Biochem. 98*, 1427−1431.
van Agthoven, A. J., Maassen, J. A., & Möller, W. (1977) *Biochem. Biophys. Res. Commun. 77*, 989−998.
Vilella, M. D., Remacha, M., Ortiz, B. L., Mendez, E., & Ballesta, J. P. G. (1991) *Eur. J. Biochem. 196*, 407−414.
Ward, L. D., Matthews, J. M., Zhang, J.-G., & Simpson, R. J. (1995) *Biochemistry 34*, 11652−11659.
Weiss, M. A., Ellenberger, T., Wobbe, C. R., Lee, J. P., Harrison, S. C., & Struhl, K. (1990) *Nature 347*, 575−578.
Yonath, A., & Berkovitch-Yellin, Z. (1993) *Curr. Opin. Struct. Biol. 3*, 175−181.
Zantema, A., Maassen, J. A., Kriek, J., & Möller, W. (1982) *Biochemistry 21*, 3077−3082.
Zhao, D., Arrowsmith, C. H., Jia, O., & Jardetzky, O. (1993) *J. Mol. Biol. 229*, 735−746.
Zinker, S. (1980) *Biochim. Biophys. Acta 606*, 76−82.
Zinker, S., & Warner, J. R. (1976) *J. Biol. Chem. 251*, 1799−1807.

BI9702400